

Synchronization in a chain of nearest neighbors coupled oscillators with fixed ends

Hassan F. El-Nashar

*Department of Physics, Faculty of Science, Ain Shams University, 11566 Cairo, Egypt
and Abdus Salam International Center for Theoretical Physics, P.O. Box 586, 34100 Trieste, Italy*

Ying Zhang and Hilda A. Cerdeira

Abdus Salam International Center for Theoretical Physics, P.O. Box 586, 34100 Trieste, Italy

Fuwape Ibiyinka A.

Federal University of Technology, Department of Physics, P.M.B. 704, Ondo State, Akure, Nigeria

(Received 31 March 2003; accepted 1 August 2003; published 24 September 2003)

We investigate a system of coupled phase oscillators with nearest neighbors coupling in a chain with fixed ends. We find that the system synchronizes to a common value of the time-averaged frequency, which depends on the initial phases of the oscillators at the ends of the chain. This time-averaged frequency decays as the coupling strength increases. Near the transition to the frozen state, the time-averaged frequency has a power law behavior as a function of the coupling strength, with synchronized time-averaged frequency equal to zero. Associated with this power law, there is an increase in phases of each oscillator with 2π jumps with a scaling law of the elapsed time between jumps. During the interval between the full frequency synchronization and the transition to the frozen state, the maximum Lyapunov exponent indicates quasiperiodicity. Time series analysis of the oscillators frequency shows this quasiperiodicity, as the coupling strength increases. © 2003 American Institute of Physics. [DOI: 10.1063/1.1611851]

Systems of interacting units represent problems in many fields, such as physics, chemistry, biology, neurophysiology, and engineering. They have been used to model phenomena as diverse as Josephson junction arrays, multi-mode lasers, vortex dynamics in fluids, biological information processes, and neurodynamics.¹⁻⁶ One of the interesting phenomena observed in these systems is that the interacting oscillators synchronize themselves to a common frequency. Particularly, these systems show an extremely complex clustering behavior as a function of the coupling strength: partial synchronization or total synchronization, phase synchronization as well as lag synchronization, etc.⁷⁻¹⁴ Although the dynamical systems describing the above mentioned phenomena are quite different, there are general features that can be described using a simple model of coupled phase equations.

I. INTRODUCTION

The vast literature in these field do not allow us to be fair, but we believe most of the well known examples can be covered by referring to Refs. 15–20, as well as to the previous references.

In spite of the extensive exploration of the dynamical behavior of coupled chaotic systems that show synchronization phenomena, many interesting features remained unknown.^{21,22} Recently, Zheng *et al.*²³ studied the complex synchronization tree of a system of oscillators with nearest neighbors interactions, modeled by

$$\dot{\theta}_i = \omega_i + \frac{k}{3} [\sin(\theta_{i+1} - \theta_i) + \sin(\theta_{i-1} - \theta_i)], \quad (1)$$

with natural frequencies ω_i selected randomly from a normal Gaussian distribution, k is the coupling strength, $i = 1, 2, \dots, N$, θ_i is the instantaneous phase and $\dot{\theta}_i$ the instantaneous frequency. Such oscillators with nearest neighbors interaction appear in Josephson junctions, laser arrays and phase-locked loops.²² These nonidentical oscillators cluster in time averaged frequency, until they completely synchronize to a common value of average frequency. Using periodic boundary conditions $\theta_{i+N} = \theta_i$, and scaling the frequencies such that

$$\frac{1}{N} \sum_{i=1}^N \omega_i = 0 \quad (2)$$

the above system (1) of N oscillators, has a critical coupling strength $k = k_c$, where for $k > k_c$, a complete frequency synchronization can be observed where $\dot{\theta}_i = 0$. In addition each θ_i is locked to a fixed value. For $k < k_c$, no phase locking can occur and $\dot{\theta}_i(t)$ is nonzero and time dependent. Frequency synchronization between the individual oscillators can be observed in the time average sense $\langle \theta_i \rangle = \langle \theta_j \rangle$, $i \neq j$, where

$$\langle \theta_i \rangle = \lim_{T \rightarrow \infty} \frac{1}{T} \int_0^T \dot{\theta}_i(t) dt. \quad (3)$$

In this case, when $k < k_c$, the system has clusters of oscillators of the same average frequencies. Reducing further the coupling strength k , the number of units of the same average frequencies decreases until finally all oscillators become with their natural frequencies through a complex structure. Also, it has been found near the critical coupling k_c (near the tran-

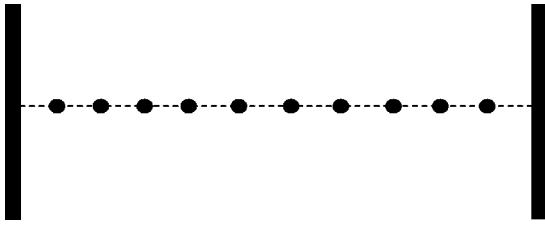


FIG. 1. Chain of oscillators with fixed ends.

sition to a common average frequency) simultaneous quantum slip features of the phases of the oscillators. The constraint (2) in the case of system (1) limits the synchronization to a zero frequency while maintaining the periodic boundary conditions. When this constraint is not used, the general features of the system will not be changed and the synchronization occurs via the same transition tree to a common frequency value

$$\omega_0 = \pm \frac{1}{N} \sum_{i=1}^N \omega_i. \tag{4}$$

If we lift the periodic boundary condition $\theta_{i+N} = \theta_i$ and at the same time two neighbor oscillators are connected to fixed ends, the ring of the oscillators becomes a chain with fixed ends. As shown in Fig. 1, first and last oscillators can be simply imagined as if they were joined to walls. Now system (1) has the property: $\theta_{i-1} = C_1$, where $i=1$ and $\theta_{N+1} = C_N$. For simplicity (1) can be written as set of three groups of equations

$$\begin{aligned} \dot{\theta}_1 &= \omega_1 + \frac{k}{3} [\sin(\theta_2 - \theta_1)] + \frac{k}{3} [\sin(C_1 - \theta_1)], \\ \dot{\theta}_i &= \omega_i + \frac{k}{3} [\sin(\theta_{i+1} - \theta_i)] + \frac{k}{3} [\sin(\theta_{i-1} - \theta_i)], \tag{5} \\ \dot{\theta}_N &= \omega_N + \frac{k}{3} [\sin(C_N - \theta_N)] + \frac{k}{3} [\sin(\theta_{N-1} - \theta_N)]. \end{aligned}$$

We will see that this system possesses quite different features and characteristics than those of a ring. We expect that, under the influence of coupling it will synchronize in frequency through a tree with the general features of that of Eq. (1), and there will be a critical value of the coupling strength at which the system possesses a common average frequency. We will see that, in spite of not being intuitive, constraint (2) will make us miss some information about system (5), that is, when $\omega_0 \neq 0$, the oscillators will synchronize to a common average frequency not equal to ω_0 . Also, as the coupling strength increases, this average-frequency will start to decay to the frozen state, where all frequencies $\dot{\theta}_i = 0$, and this decay will show unexpected properties. We will study how all this occurs. In particular, we will show that the average frequency synchronization occurs at a value $\langle \dot{\theta}_i \rangle \neq \omega_0 \neq 0$, i.e., there is a critical value of the coupling strength, we call it k_s , where frequency synchronization between all oscillators occurs while the phases of the oscillators are not locked. At k_s , the value of $\langle \dot{\theta}_i \rangle$ depends on the phases of the oscillators at the ends. We will also show that the value of k_c , where the

system freezes and $\dot{\theta}_i = 0$, depends on the constraint parameter (4) and how much ω_0 differs from zero. It should be noted that when $\omega_0 = 0$ is used, then $k_s = k_c$ also for the chain with fixed ends. Finally we will show that at k_s , although the system has a common average frequency, it does not show phase slip features. However, these phase slip features appear near the critical value k_c when the system goes to the frozen state. Near k_c each phase $\theta_i(t)$ of the oscillators will have an intermittent sequence of 2π jumps. In this region near k_c we can also define a power law behavior for the dependence of τ , which is the time of duration of each phase slip, and $\langle \dot{\theta}_i \rangle$, on $[k_c - k]$. We aim at understanding the physical origin of such intermittency near the transition and how this power law behavior is related to the phase jumps.

This paper is organized as follows: in Sec. II, we show the features of the frequency synchronization of system (5). In Sec. III, the temporal behavior of frequencies of the coupled oscillators is investigated. Section IV is devoted to explore the phase slip near the frozen state. In Sec. V a conclusion is given.

II. FEATURES OF FREQUENCY SYNCHRONIZATION

In this section we study the behavior of a chain of oscillators with fixed ends. In Fig. 2, we show the time averaged frequency as a function of the coupling strength k for a system of 16 oscillators. The main part of Fig. 2(a) shows the synchronization tree, which has a complex structure. We notice clustering in frequency occurs, with the size of the clusters increasing, until at $k = k_s$, the oscillators form a coherent state in time-averaged frequency, with an average frequency different from ω_0 . It is observed that the formation of clusters of the same average frequency occurs due to the nearest neighbors interactions, where elements which are closer in space and closer in initial frequencies cluster first [number of oscillators are indicated in Fig. 2(a)].^{24,25} We see from Fig. 2(a) that, increasing the coupling strength, the value of the average frequency decays. The rate of decay becomes stronger as k increases until the average frequency reaches zero at k_c . For $k \geq k_c$ the system is frozen with $\dot{\theta}_i = 0$. We observe in Fig. 2(b) the same feature as Fig. 2(a) but for smaller coupling strength. It is interesting to understand why the synchronization frequency at k_s occurs at a lower value than ω_0 and why the value of the average frequency decays when the coupling strength increases. A clear answer for such questions will be left to the next section since the exploration needs some investigation of the temporal behavior of system (5) for $k \geq k_s$. In the inset of Fig. 2(b) we show the behavior of ω_0 versus k_c for different distributions of initial frequencies. Notice that for $\omega_0 = 0$, k_c has its minimum value and it coincides with k_s . The synchronization tree is independent of the initial conditions for the phases for all values of k , except in the vicinity of k_c , the value of the coupling strength for which $\dot{\theta} = 0$. In Fig. 2(a) (main frame and inset) another feature is shown, which is the dependence of the value of k_c on the initial distributions of the phases $\Delta\theta_{ij} = |\theta_i - \theta_j|$ in the interval $[0, 2\pi]$. Notice that for different initial distributions of the phases, the rate of the decay of $\langle \dot{\theta}_i \rangle$ varies changing the value of the critical coupling k_c . In

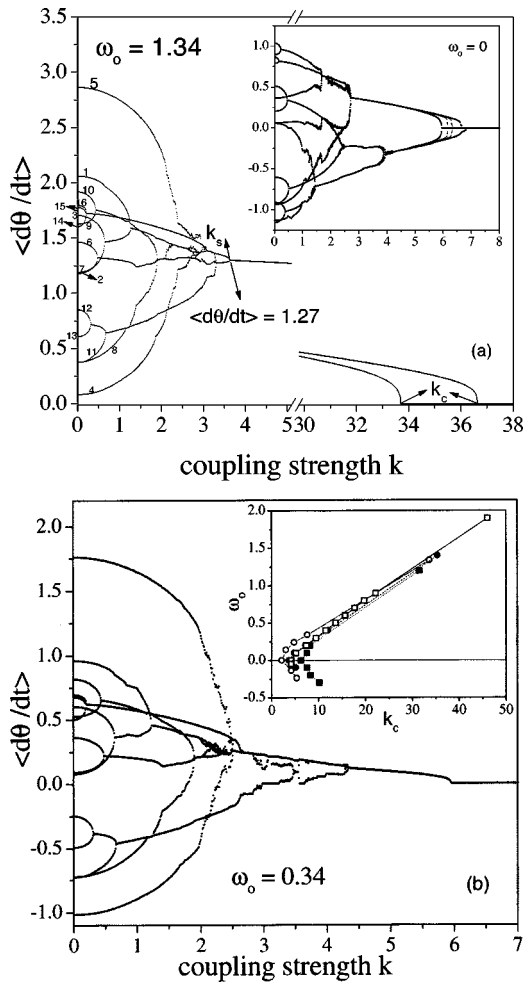


FIG. 2. Synchronization tree of time-averaged oscillators frequencies versus the coupling strength k . (a) for $\omega_0=1.34$ (number of oscillators are indicated); (b) for $\omega_0=0.34$. The inset of (a) shows another tree for $\omega_0=0$ and the dependence of k_c at initial phases as well as in (a). The inset of (b) shows the change of the constraint ω_0 versus k_c .

the inset of Fig. 2(b) we show the same dependency of k_c on initial phases for another set of the distribution of $\Delta\omega_{ij} = |\omega_i - \omega_j|$. Figure 2(b) has been obtained with the same set of initial conditions for the distribution of phases $\Delta\theta_{ij} = |\theta_i - \theta_j|$ in the interval $[0, 2\pi]$, and for unevenly spaced initial frequencies $\Delta\omega_{ij}$, i.e, different values of the constraint parameter ω_0 . In order to understand why k_c depends on the initial conditions of phases, we plot Fig. 3. This figure shows the dependence of k_c on the initial phases of the two oscillators at the ends of the chain for $\omega_0=0$. In fact we choose only the first and the last oscillators since according to Eq. (5) the frequencies of these two oscillators have a stronger dependence on the phases of the oscillators at the ends than any other oscillators in the chain, which have frequencies depending on the phase differences of neighboring oscillators. On the other hand the initial phases of the two oscillators at the ends represent two constants in the interval $[0, 2\pi]$, which can be replaced by any two arbitrary constants in the same interval, as will be clear in the next section.

As we have seen from Fig. 2 by inspection of the synchronization tree, there appears to be a universal behavior of the time-averaged frequency of the oscillators in the vicinity of k_c . We have studied this region carefully for many values of the constraint parameter ω_0 , for different distributions of initial frequencies $\Delta\omega_{ij}$, and for different initial conditions for the phases $\Delta\theta_{ij}$. The results are plotted in Fig. 4 where a perfect scaling can be observed and the time-averaged frequency scales with the coupling strength as $\langle \dot{\theta}_i \rangle \sim |k_c - k|^{0.5}$. The exponent has been calculated within an error ± 0.02 . This kind of exponent gives an indication of the occurrence of a saddle node instability. This transition may indicate that in the vicinity of k_c there is a quasiperiodic motion and the system goes to a periodic motion and each oscillator locks in phase at k_c .^{21,23,26} To figure out such characteristics, we will calculate the maximum Lyapunov exponent (at the end of this section) to see how it behaves with

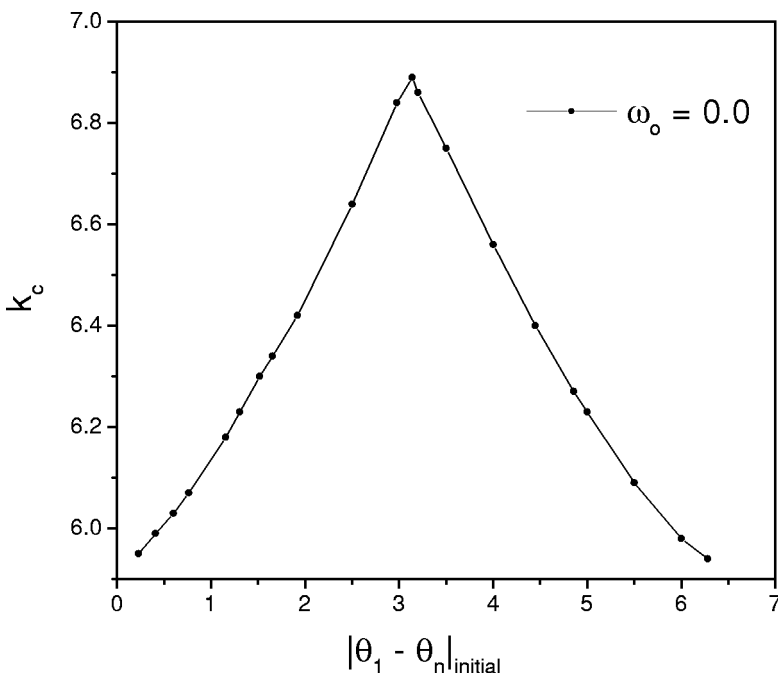


FIG. 3. Dependence of k_c on the initial values of phases of the first and the N th oscillators, which are representing two arbitrary constant values in the interval $[0, 2\pi]$.

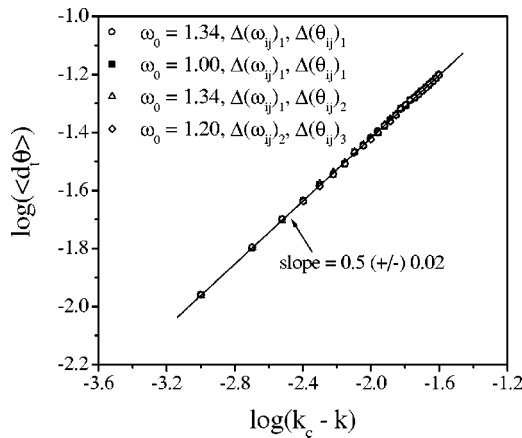


FIG. 4. log-log plot of the average frequencies of oscillators versus $|k_c - k|$.

increasing k . In addition, in the next section we shall study some features of the frequencies $\dot{\theta}_i$ as a function of time, which serve to clarify the scenario.

In order to look at the qualitative picture of the phases of oscillators under the influence of coupling, we have plotted the average of Kuramoto order parameter $\langle R \rangle$,²⁸ Fig. 5, where

$$R = \frac{1}{N} \left| \sum_{j=1}^N e^{i\theta_j} \right|. \quad (6)$$

For $\omega_0=0$, $\langle R \rangle$ quickly increases exponentially after k_c , and there is no complete synchronization in phase since $\langle R \rangle \neq 1$ which means that all the oscillators do not have the same phase. However, the exponential growth after k_c indicates that the oscillators may lock in phase difference. For $\omega_0 \neq 0$ it seems that $\langle R \rangle$ always increases exponentially after k_c . Figure 5 also shows that when $\omega_0 \neq 0$, there is an indication of a loss of coherence of the phase locked state after k_s . This is clearly observed when the shift of ω_0 from zero becomes large. This may indicate that system (5) tries to go to a phase lock state and frequency synchronization at k_s but

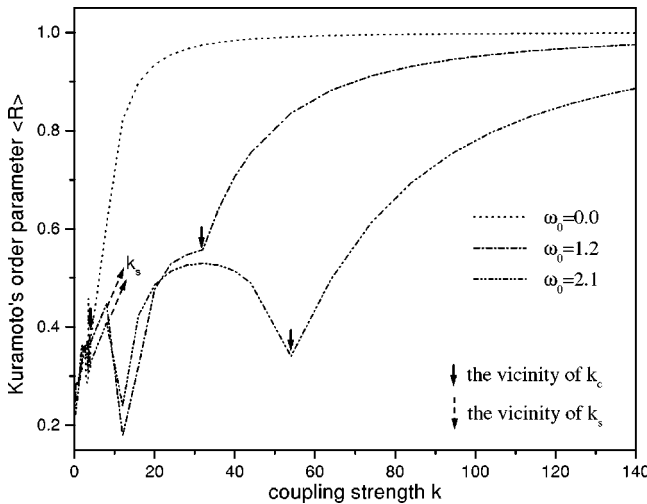


FIG. 5. Order parameter $\langle R \rangle$ versus the coupling strength k for different values of the constraint ω_0 .

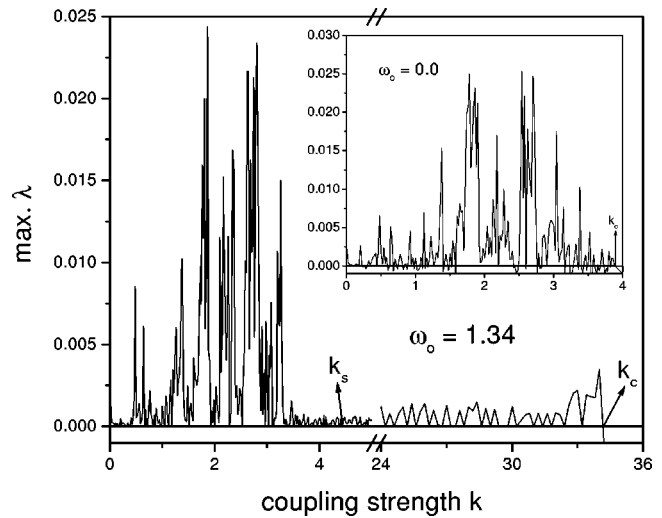


FIG. 6. Maximum Lyapunov exponent for $\omega_0=1.34$. The inset shows the maximum Lyapunov exponent for $\omega_0=0$.

it fails as the coupling strength increases. It also indicates that oscillators may have a quasiperiodic motion until the coupling strength arrives to the value of k_c . In order to see the behavior of the chaotic, quasiperiodic and periodic motions of the system, we have plotted in Fig. 6 the maximum Lyapunov exponent versus the coupling strength. We observe that the system is chaotic during the transition tree and, while clusters of oscillators of common average frequency are formed and it goes to quasiperiodic motion near k_s . The reason why system (5) is chaotic in the interval $(0 < k \leq k_s)$ was thoroughly explained in Refs. 21, 23. We do not expect the maximum Lyapunov exponent to be negative and the system to be periodic after k_s (see also the observation from Fig. 5). The only case when the maximum Lyapunov exponent is negative at k_s , is when $\omega_0=0$. This is clearly observed from the inset of Fig. 6. As shown from Fig. 6 (main frame), the fluctuation of the maximum Lyapunov exponent around zero near k_s is small, which may mean that the system tries to undergo a quasiperiodic to periodic transition at k_s . However, it fails and the fluctuation in the maximum Lyapunov exponent increases as k increases until the vicinity of k_c . It is therefore interesting to investigate the dynamics of the motion of the oscillators of system (5). The study of the spatiotemporal behavior will help us to interpret what happens in the interval $k_s \leq k \leq k_c$. Particularly, it gives a deep insight towards the understanding of how the oscillators follow the two oscillators at the ends of the chain and how the frequency decays to the frozen state following a power law behavior near the vicinity of k_c .

III. TEMPORAL BEHAVIOR OF FREQUENCIES OF THE OSCILLATORS

In this section we do further quantitative analysis and study the temporal behavior of the frequencies of the oscillators at several values of $k \geq k_s$. This study has been done in order to understand some of the observed features in the synchronization tree for $k \geq k_s$. Particularly, we try to find answers to the following questions: “Why do all oscillators

at k_s have a common average frequency $\langle \dot{\theta}_i \rangle \neq \omega_0$? Why does this average frequency decay as the coupling strength increases? And, why, near the critical coupling k_c , does there exist a power law behavior for the value of $\langle \dot{\theta}_i \rangle$ as a function of k , when k approaches k_c and the system goes to the frozen state?"

According to Eq. (5) at k_s all oscillators have a common average frequency value, which is given by

$$\langle \dot{\theta}_i \rangle = \langle \dot{\theta} \rangle = \frac{1}{N} \left[\sum_{i=1}^N \omega_i + \frac{k}{3} \langle \sin(C_1 - \theta_1) \rangle + \langle \sin(C_N - \theta_N) \rangle \right]. \tag{7}$$

To facilitate the discussion let us define

$$A_i = \frac{k}{3} \langle \sin(\theta_{i+1} - \theta_i) \rangle, \tag{8}$$

$$B_i = \frac{k}{3} \langle \sin(\theta_{i-1} - \theta_i) \rangle,$$

such that for each oscillator $\dot{\theta}_i$ is given by the addition of the three quantities ω_i , A_i and B_i . A_i and B_i have the following properties: $A_i = -B_{i+1}$ for $i = 1, 2, \dots, N-2$ and $A_{N-1} = -B_N$. Therefore, at k_s all terms cancel each other except B_1 and A_N . It is clear from the above equation that $\dot{\theta}_i(t)$ depends on the phases of the two oscillators, $\theta_1(t)$ and $\theta_N(t)$, at the ends of the chain, since taking $C_1 = C_N = 0$ does not change the behavior of the synchronization tree. The values of C_1 and C_N can be the initial phases of the first and N th oscillators or can take any values in the interval $[0, 2\pi]$. Now, what appears to be a dependence of k_c on the initial phases is due to the values of phases next to the fixed ends.

Now, let us try to find an answer to the first question. The behavior of the two terms in Eq. (7) which depend on the phases of the first and last oscillators should be negative on the time-averaged in order to reduce the value of ω_0 to the value of $\langle \dot{\theta}_i \rangle$ at k_s (see Fig. 2). This behavior is due to the fact that $\theta_1(t)$ and $\theta_N(t)$ fluctuate to lower and higher values around a given average, independent of the values of C_1 and C_N . The fluctuations of phases may be towards the lower value more than the higher such that finally the average values that contribute to $\langle \dot{\theta}_i \rangle$ are negatives. In order to see this clearly, we look at the two parts of Eq. (7) which are coming originally from the second term of the frequency of the first oscillators and the first term of the frequency of the last oscillator, B_1 and A_N , respectively, we have plotted the time series of these two parts at k_s , as shown in Figs. 7(a) and 7(b). This figure shows a part of the temporal behaviors of B_1 at Fig. 7(a) and B_{16} at Fig. 7(b), which are carrying the same features in the whole range of time. It is shown from Figs. 7(a) and 7(b) that the two parts fluctuate around a given average. The fluctuations towards lower values reach practically the same value after each revolution while the fluctuation towards a positive value do not reach the same strength after each revolution of the oscillators. Therefore, each part as shown in Figs. 7(a) and 7(b) has an average value which is negative as shown by the dotted lines. This finally reduces

the average value of each part to a final negative value, which in turn reduces the value of ω_0 to the value of $\langle \dot{\theta}_i \rangle$ as observed from Fig. 2. We have checked this behavior with several values of C_1 and C_N , and we found the same behavior. The only change occurs to the value of k_c as indicated in the previous section. It is clearly seen from Eq. (7) that due to different values of C_1 and C_N , we find different values of k_c (see Fig. 3) for the same $\Delta\omega_{ij}$.

Now we arrive to answer the second question, i.e; we try to understand why the average frequency $\dot{\theta}_i$ decays to zero. Figures 7(a)–7(h) show the part of the time series of the two contributions to the phases of oscillators 1, 8, 13 and 16. We have chosen these oscillators in order to find a reason for the decay in the average frequency that may pass through the oscillators due to the nearest neighbor interactions. This can be done examining the behavior of each part for the first oscillator, one of the middle oscillators near to the first, one of the middle oscillators which is far from both first and N th oscillators, one of the oscillators which is closer to the N th oscillator and finally the N th oscillator. As shown from Fig. 7, it is clear that both oscillators at the ends of the chain have the higher fluctuations in frequency among all oscillators. Due to the nearest neighbor interactions these fluctuations are transferred (by diffusion) to other oscillators, which weaken as we go towards the center of the chain, and they approximately vanish in the center of the chain (e.g., 8). Therefore, the situation at k_s could be as follows: oscillators at the middle synchronize and would prefer to go from a state of quasiperiodic to a state of periodic motion while oscillators at the two ends of the chain cannot match this motion. As k increases the oscillators at the ends, which possess large fluctuations in their frequency, drive other oscillators to follow them. As the coupling strength increases, we expect that the fluctuations in the frequencies of the two end oscillators increase and their effect will extend to the middle oscillators through the local interactions. This in turn drives the other oscillators frequencies to fluctuate stronger around the average. Figures 8(a)–8(e) show the A and B parts of oscillators 1, 3 and 8 (since 13 and 16 have similar features on the average as 3 and 1, respectively). As shown from this figure the fluctuations in the frequency of the first oscillator increases and its larger contribution comes from B_1 , which lowers the value of the average frequency. Due to the diffusive interaction between the oscillators, the fluctuations travel along the chain until finally drives A_8 and B_8 to fluctuate around an average which contribute to lower the average frequency $\langle \dot{\theta}_8 \rangle$ from being equal to ω_o as k increases. This observation is valid for all oscillators in the chain. It is shown from Fig. 8 that the contribution to the average frequency of each oscillator is due to both terms A and B . This contribution reduces the value of the average frequency. As k increases we expect that the fluctuations in frequencies become stronger and the reduction in the average frequency increases. In order to see this clearly, we plot in Fig. 9(a) $\dot{\theta}(n)$ versus $\dot{\theta}(n+1)$ for $k=10$. We find at $k=k_s=4.51$ a similar behavior to that in Fig. 9(a). This figure shows the return map of the frequency for oscillators 1, 4, 8, 12, and 16. As we go to the middle of the chain, the fluctua-

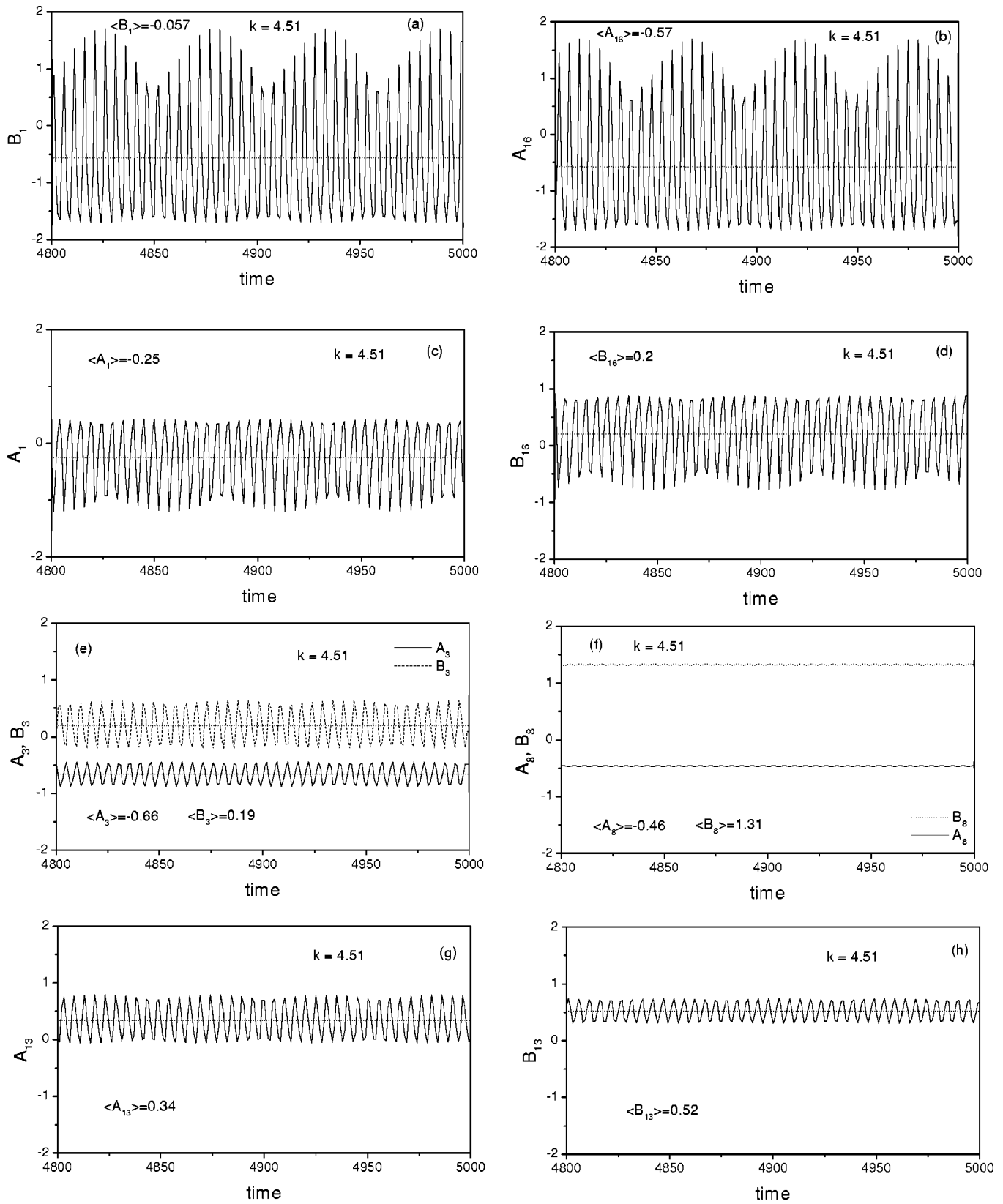


FIG. 7. Parts of the time series of the the different phase parts as in (7), at $k = k_s = 4.51$, for several oscillators.

tions are reduced until they approximately vanish at 8 while the others near to the ends and the two at the ends have higher fluctuations. Also, it is indicated from Fig. 9(b) that as k increases, the fluctuation of each frequency increases. In

addition, there is a quasiperiodic motion as shown in Fig. 9. It is noticed also that the center of oscillation (average value) is shifted towards a lower value as k increases.

In fact, system (5) has characteristics of nonuniform os-

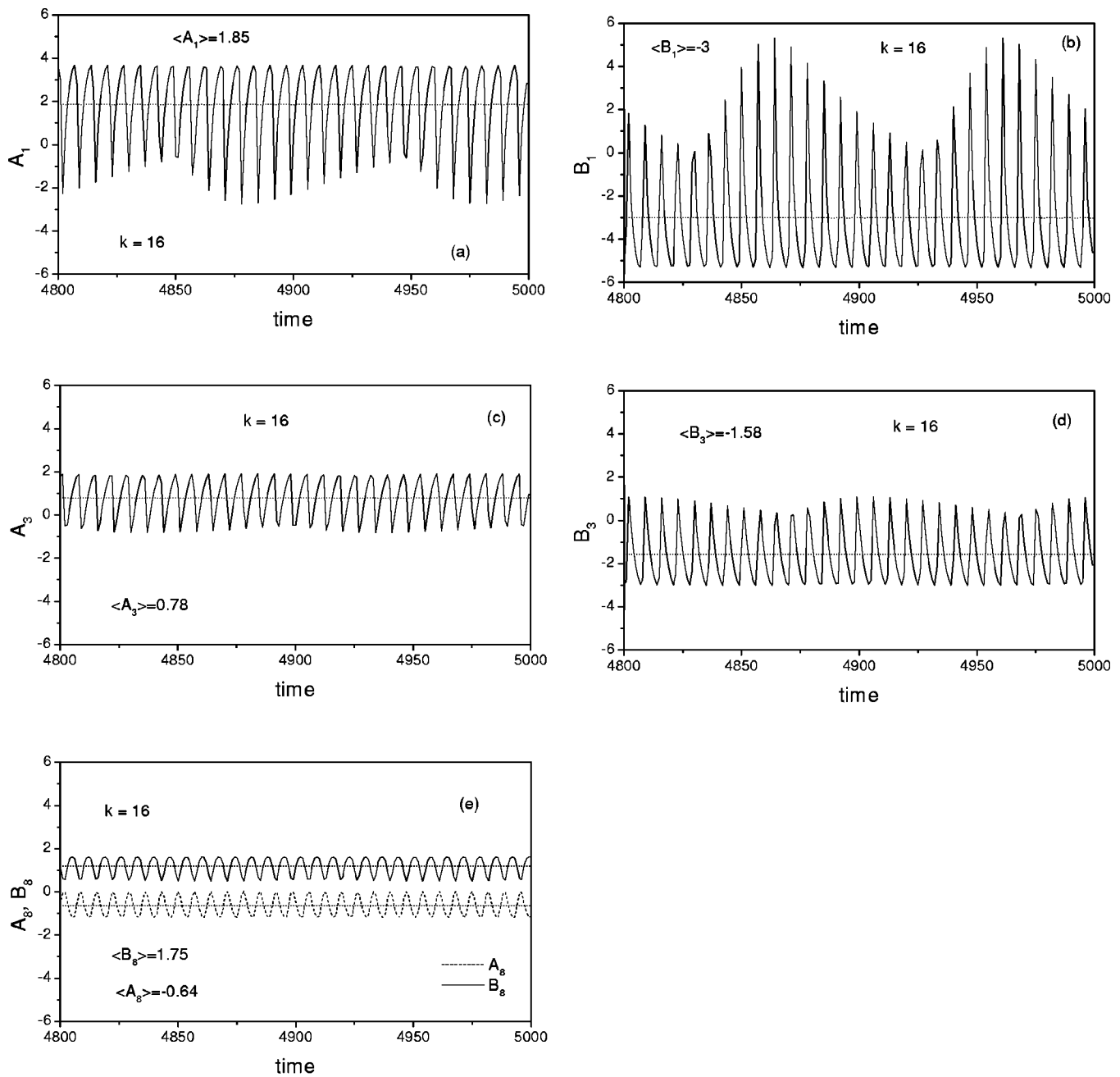


FIG. 8. Parts of the time series of the different phase parts as in Eq. (7), at $k = 16$, for several oscillators.

oscillators which have fast and slow frequencies during each revolution. It seems that at k_s , the oscillators at the two ends oscillate faster and then slower than other oscillators while the oscillator(s) in the middle have an approximately uniform oscillation. As the coupling strength increases, the oscillators at the ends influence the others to move with quasi-periodic motion (since they drive other oscillators to have fast and slow motion during each revolution in time). As k increases further, the oscillators have a harder change in instantaneous velocities during each revolution. At the same time the center of oscillation moves closer to zero. We expect that as k increases to be in the vicinity of k_c , the center of oscillation moves towards the vicinity of zero. The situation is similar to that of a nonuniform oscillator with a slow passage due to the vicinity of a saddle-node bifurcation. There-

fore, there is a saddle-node remnant or ghost which leads to this slow passage.²⁹ In order to examine such behavior we investigate the time series of each oscillator's frequency. Figures 10(a)–10(c) show parts of this time series of oscillators 1, 4 and 8. It is seen that at k_s or larger, the instantaneous velocity of the first oscillator has a slow motion during each revolution which repeats itself with the same magnitude while it has a fast velocity with different magnitudes during different revolutions. Other oscillators in the middle of the chain have the same feature but with less variation in magnitudes. As k increases, the oscillators have a stronger slowing down during each revolution. At the vicinity of k_c , the oscillators approximately stop moving for a while and then move fast in a sudden jump. The duration of the time of each stop (off state) increases very fast as we approach k_c . Now

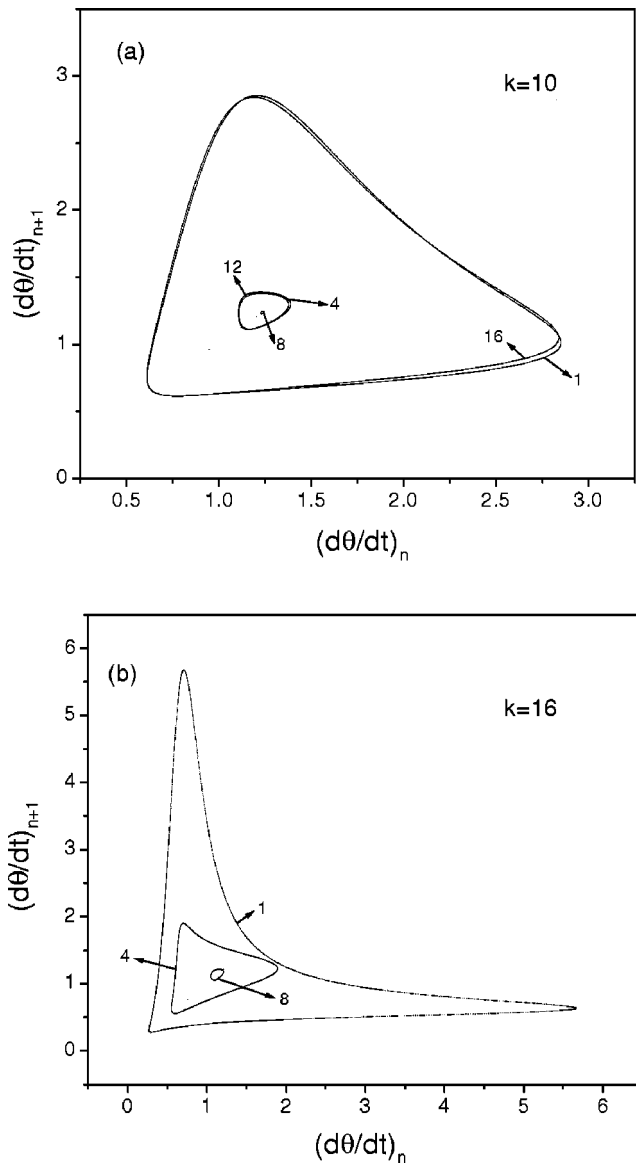


FIG. 9. Maps of θ_n to θ_{n+1} for (a) $k=10$ and (b) $k=16$.

we are closer to answer the third question, since the square root scaling law for $\langle \dot{\theta}_i \rangle$ as a function of $(k_c - k)$ is pointing to a saddle-node transition. This we do in the next section.

IV. QUANTIZED PHASE SLIP NEAR THE FROZEN STATE

As indicated in the previous section, near the vicinity of k_c , there exists a kind of synchronized firing of motion. That is to say, we find a simultaneous on-off state [see Fig. 10(c)], where all oscillators are in the off state and then simultaneously burst to the on state. As k gets closer to k_c , the time τ between two successive bursts becomes longer. At $k=k_c$, τ goes to infinity. In order to see such two states (on-off) during the increase of k value to be closer to k_c , we plot Figs. 11(a) and 11(b). It is shown from Fig. 11(a) that the evolution of the phases (for example of first oscillator) varies monotonically until we arrive to $k=33.07$. For values of $34.07 \leq k \leq k_c$, we find a clear presence of on-off states and the length in time of each state becomes longer as we go

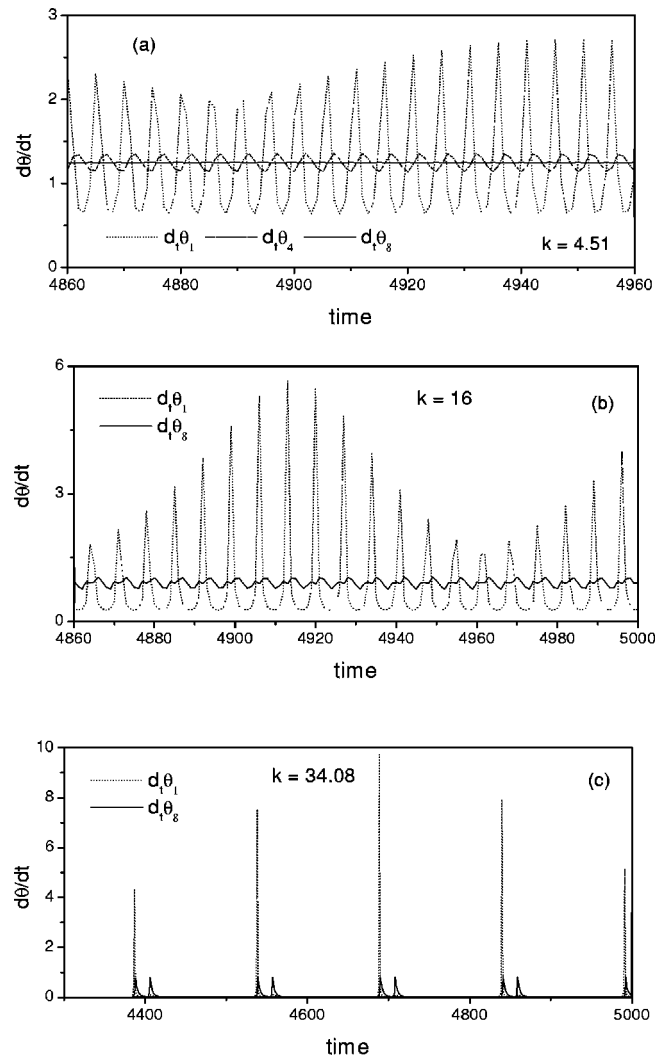


FIG. 10. Parts of the time series of the instantaneous velocities for several oscillators at (a) $k=k_s=4.51$, (b) $k=16$, and (c) $k \sim 34.08$.

closer to $k_c=34.1$ [see Fig. 11(b)]. In order to examine the behavior of the duration in time of (on-off) states versus $k_c - k$ we plot Fig. 12. As shown from Fig. 12, for two values of ω_0 , the scaling law takes the form $\tau \sim (k_c - k)^{-1/2}$. Therefore, in order to relate this scaling law to that of $\langle \dot{\theta}_i \rangle \sim (k_c - k)^{1/2}$, we may say that for $|k - k_c| \ll 1$, there is a saddle-node instability leading to the slow passage and a saddle-node remnant appears, since the oscillation is affected by the nonlinear term of phases for each oscillator. Such effect, for $k \geq k_c$ does not affect the stability of the system. However, for a value of k near the vicinity of k_c the stable fixed points do not exist but they feel a saddle-node ghost. For the saddle-node bifurcation we can write the universal form³⁰ which is given by

$$\dot{x} = (k_c - k) + x^2. \tag{9}$$

The time τ takes the form

$$\tau \sim \int_0^\infty \frac{dx}{(k_c - k) + x^2} = \frac{\pi}{2(k_c - k)^{1/2}}. \tag{10}$$

For the saddle-node bifurcation, we find that $\langle \dot{\theta}_i \rangle \sim (k_c - k)^{1/2}$. The inset of Fig. 11(b) shows the jumps by 2π of the

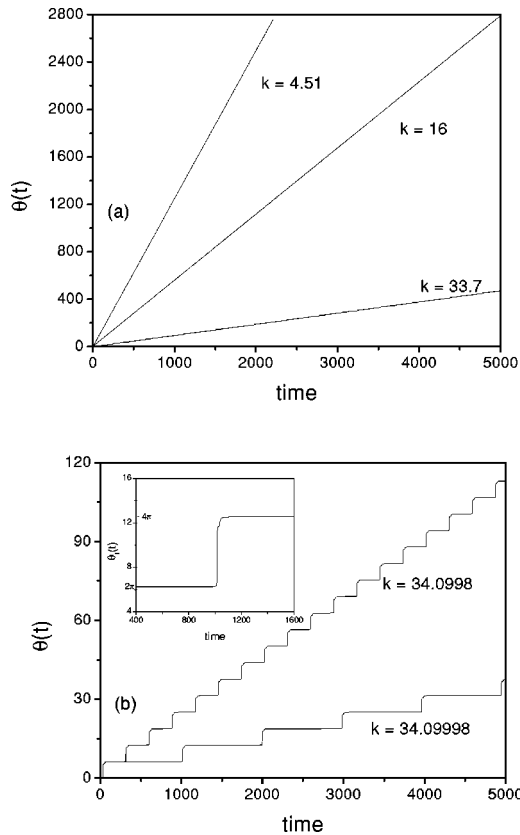


FIG. 11. Evolution of phase for the first oscillator for different values of k . (a) shows the monotonic variation of θ with time until $k = 33.7$; (b) shows the phase slip in the vicinity of k_c . The inset of (b) shows in the vicinity of k_c there exists a jump by $s\pi$ for the values of phases.

phases during each revolution. Qualitatively, we can relate the behavior near k_c to a behavior of the motion of an overdamped particle in a potential, which has a series of local minima. Above the bifurcation ($k > k_c$), the particle is trapped to one of this minima permanently. For $k < k_c$, there is no stable fixed point and the particle slides 2π periodically.²⁶ The phenomena was reported for the case of two noninteracting externally driven oscillators. Later, Boc-

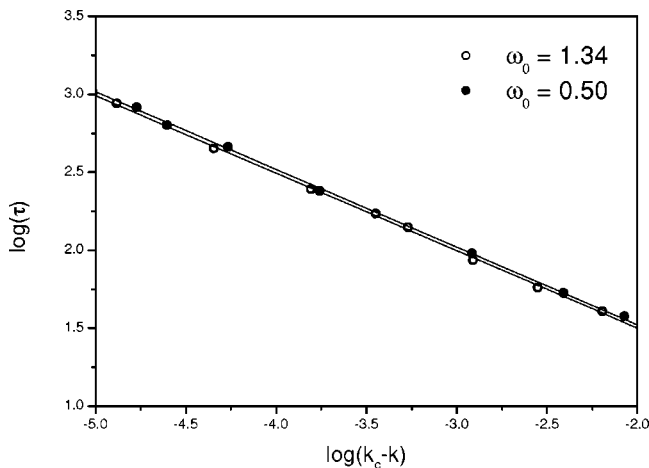


FIG. 12. \log - \log plot of the duration time τ versus $k_c - k$ for two different values of ω_0 .

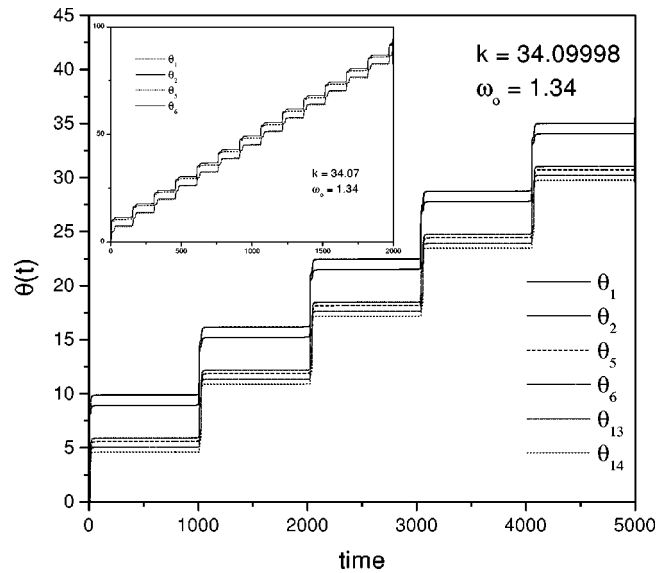


FIG. 13. The evolution of θ with time near k_c . The main part and the inset show the phase differences between adjacent and nonadjacent oscillators to represent that the phases as k approaches k_c , phases are going to be locked.

caletti *et al.*²⁷ reported experimental evidence for an equivalent system. This is the first time, to our knowledge, when a collective phase slip is reported. It will be interesting to see whether or not the effect of a forcing frequency in a system with a large number of oscillators will have the same kind of scaling. It is not clear without further evidence that there will be a transition to a superlong laminar period intermittency, and it is not within the scope of this work to engage in this calculation.

Figure 13 shows the evolution of phases of several oscillators near the vicinity of k_c . It is shown from this figure that the phase difference between the oscillators are kept fixed at nonzero value. Also, it is shown that the phase difference between adjacent oscillators is smaller than between nonadjacent. The inset of Fig. 13 shows the same features for another value of k . Both, the main and the inset, of Fig. 13 show that as k approaches k_c , the phases are going to take a constant value (phase lock) and the differences between phases are going to be constant. We can relate this finding to what is found in the Kuramoto order parameter $\langle R \rangle$ (see Fig. 3), where we found that the order parameter is not equal to unity at k_c .

V. CONCLUSION

In conclusion, while studying the behavior of phase coupled oscillators with nearest neighbors coupling in a fixed end chain, we have seen that the system has a common average frequency synchronization at a value of the coupling strength, we call it k_s , which is not equal to the value of $\omega_0 = (1/N) \sum_{i=1}^N \omega_i$. This common average frequency decays under the influence of coupling to a zero value (frozen state) at k_c . During the interval $k_s \leq k \leq k_c$, the system remains quasiperiodic. This quasiperiodicity is shown by the maximum Lyapunov exponent, as well as the time series of frequencies of oscillators. Also, we found a universal scaling law in the time-averaged frequency as a function of the cou-

pling strength at the transition to the frozen state. The time series of frequencies and phases of the oscillators relate this power law to a saddle-node bifurcation at k_c . For $k < k_c$, a saddle-node remnant appears which leads to the presence of on-off states of the frequencies. This behavior shows a quantized phase slip during the change between the two states. The time in between slips has a power law scaling. We have shown that there is no total phase synchronization for finite values of $k < k_c$. In the vicinity of k_c each phase is locked to a certain value and the phase difference between two oscillators does not equal zero. We have also found that each phase of oscillators has a quantized jump by an amount of 2π near the vicinity of k_c . We relate qualitatively this behavior to the behavior of the motion of an overdamped particle in a potential with a series of local minima. However, in order to be sure about such argument we need to study the behavior of the oscillators in such a potential near k_c . In addition, we need to study the region near k_c very carefully before making any quantitative arguments, which is outside the scope of this manuscript.

ACKNOWLEDGMENTS

The authors thank D. H. Zanette for fruitful discussions. H.F.E. thanks MPIPKS for support during part of this work, Yang Hungliu and J. Dorniac at MPIPKS for discussions. H.A.C. acknowledges local hospitality from the MPIPKS.

- ¹A.S. Pikovsky, G. Osipov, M.G. Rosenblum, M. Zaks, and J. Kurths, *Phys. Rev. Lett.* **79**, 47 (1997).
- ²D. Dominguez and H.A. Cerdeira, *Phys. Rev. Lett.* **71**, 3359 (1993).
- ³G. Perez, C. Pando-Lambruschini, S. Sinha, and H.A. Cerdeira, *Phys. Rev. A* **45**, 5469 (1992).
- ⁴Y. Kuramoto, *Chemical Oscillations, Waves and Turbulences* (Springer, Berlin, 1984).
- ⁵A.T. Winfree, *Geometry of Biological Time* (Springer, New York, 1990).
- ⁶K. Wiesenfeld, P. Colet, and S.H. Strogatz, *Phys. Rev. Lett.* **76**, 404 (1996).

- ⁷C.M. Gray, P. Koenig, A.K. Engel, and W. Singer, *Nature (London)* **338**, 334 (1989).
- ⁸K. Kaneko, in *Statistical Physics (STATPHYS 19), Proceedings of the 19th IUPAP International Conference on Statistical Physics*, Xiamen, China, edited by B.-L. Hao (World Scientific, Singapore, 1996), p. 338.
- ⁹P. Hadley, M.R. Beasley, and K. Wiesenfeld, *Phys. Rev. B* **38**, 8712 (1988).
- ¹⁰M.N. Lorenzo, I.P. Marino, V. Perez-Munizuri, M.A. Matias, and V. Perez-Villar, *Phys. Rev. E* **54**, R3094 (1996).
- ¹¹K. Otsuka, *Nonlinear Dynamics in Optical Complex Systems* (Kluwer, Dordrecht, 2000).
- ¹²G. Hu, Y. Zhang, H.A. Cerdeira, and S. Chen, *Phys. Rev. Lett.* **85**, 3377 (2000).
- ¹³Y. Zhang, G. Hu, H.A. Cerdeira, S. Chen, and Y. Yao, *Phys. Rev. E* **63**, 026211 (2001).
- ¹⁴Y. Zhang, G. Hu, and H.A. Cerdeira, *Phys. Rev. E* **64**, 037203 (2001).
- ¹⁵H. Haken, *Brain Dynamics: Synchronization and Activity Patterns in Pulse-Coupled Neural Nets with Delays and Noise* (Springer, Berlin, 2002).
- ¹⁶P.A. Tass, *Phase Resetting in Medicine and Biology* (Springer, Berlin, 1999).
- ¹⁷M. Golubitsky and E. Knobloch, eds., "Bifurcation, Patterns and Symmetry," special issue of *Physica D* **143** (2000).
- ¹⁸C.W. Wu, *Synchronization in Coupled Chaotic Circuits and Systems* (World Scientific, Singapore, 2002).
- ¹⁹S. Boccaletti, J. Kurths, G. Osipov, D.J. Valladares, and C.S. Zhou, *Phys. Rep.* **366**, 1 (2002).
- ²⁰A. Pikovsky, M. Rosenblum, and J. Kurths, *Synchronization: A Universal Concept in Nonlinear Sciences* (Cambridge University Press, Cambridge, 2001).
- ²¹Z. Zheng, B. Hu, and G. Hu, *Phys. Rev. Lett.* **81**, 5318 (1998).
- ²²D. Topaj and A. Pikovsky, *Physica D* **170**, 118 (2002).
- ²³Z. Zheng, B. Hu, and G. Hu, *Phys. Rev. E* **62**, 402 (2000).
- ²⁴H.F. El-Nashar, A.S. Elgazzar, and H.A. Cerdeira, *Int. J. Bifurcation Chaos Appl. Sci. Eng.* **12**, 2945 (2002).
- ²⁵H.F. El-Nashar, *Int. J. Bifurcation Chaos Appl. Sci. Eng.* (to be published).
- ²⁶K.J. Lee, Y. Kwak, and T.K. Lim, *Phys. Rev. Lett.* **81**, 321 (1998).
- ²⁷S. Boccaletti, E. Allaria, R. Meucci, and F.T. Arecchi, *Phys. Rev. Lett.* **89**, 194101 (2002).
- ²⁸S.H. Strogatz, *Physica D* **143**, 1 (2000), and references therein.
- ²⁹S.H. Strogatz, *Nonlinear Dynamics and Chaos* (Perseus, Cambridge, MA, 1994).
- ³⁰Y. Pomeau and P. Manneville, *Commun. Math. Phys.* **74**, 189 (1980).